



## Hagnifinder: Recovering magnification information of digital histological images using deep learning

Hongtai Zhang <sup>a</sup>, Zaiyi Liu <sup>b,c,d</sup>, Mingli Song <sup>a,e,\*</sup>, Cheng Lu <sup>b,c,d,\*\*</sup>

<sup>a</sup> School of Computer and Cyber Sciences, Communication University of China, Beijing 100024, China

<sup>b</sup> Department of Radiology, Guangdong Provincial People's Hospital (Guangdong Academy of Medical Sciences), Southern Medical University, Guangzhou 510080, China

<sup>c</sup> Medical Research Institute, Guangdong Provincial People's Hospital (Guangdong Academy of Medical Sciences), Southern Medical University, Guangzhou 510080, China

<sup>d</sup> Guangdong Provincial Key Laboratory of Artificial Intelligence in Medical Image Analysis and Application, Guangzhou 510080, China

<sup>e</sup> State Key Laboratory of Media Convergence and Communication, Communication University of China, Beijing 100024, China



### ARTICLE INFO

**Keywords:**

Histology images  
Magnification prediction  
Regression model  
Deep learning

### ABSTRACT

**Background and objective:** Training a robust cancer diagnostic or prognostic artificial intelligent model using histology images requires a large number of representative cases with labels or annotations, which are difficult to obtain. The histology snapshots available in published papers or case reports can be used to enrich the training dataset. However, the magnifications of these invaluable snapshots are generally unknown, which limits their usage. Therefore, a robust magnification predictor is required for utilizing those diverse snapshot repositories consisting of different diseases. This paper presents a magnification prediction model named Hagnifinder for H&E-stained histological images.

**Methods:** Hagnifinder is a regression model based on a modified convolutional neural network (CNN) that contains 3 modules: Feature Extraction Module, Regression Module, and Adaptive Scaling Module (ASM). In the training phase, the Feature Extraction Module first extracts the image features. Secondly, the ASM is proposed to address the learned feature values uneven distribution problem. Finally, the Regression Module estimates the mapping between the regularized extracted features and the magnifications. We construct a new dataset for training a robust model, named Hagni40, consisting of 94 643 H&E-stained histology image patches at 40 different magnifications of 13 types of cancer based on The Cancer Genome Atlas. To verify the performance of the Hagnifinder, we measure the accuracy of the predictions by setting the maximum allowable difference values (0.5, 1, and 5) between the predicted magnification and the actual magnification. We compare Hagnifinder with state-of-the-art methods on a public dataset BreakHis and the Hagni40.

**Results:** The Hagnifinder provides consistent prediction accuracy, with a mean accuracy of 98.9%, across 40 different magnifications and 13 different cancer types when Resnet50 is used as the feature extractor. Compared with the state-of-the-art methods focusing on 4–5 levels of magnification classification, the Hagnifinder achieves the best and most comparable performance in the BreakHis and Hagni40 datasets.

**Conclusions:** The experimental results suggest that Hagnifinder can be a valuable tool for predicting the associated magnification of any given histology image.

### Introduction

Until now, histology image examination was still the gold-standard for most tumor diagnosis. The traditionally used H&E staining stains the nuclei blue while extracellular materials pink to enhance the visibility of tissues.<sup>1,2</sup> Morphological features of stained tissue were examined at several different magnification levels to help a pathologist understand the current specimen's status.<sup>3</sup> The level of magnification, as important information of digital pathological images, depends on the magnification of the optical microscope objective lens.<sup>4</sup> More areas could be observed at low

magnifications, which facilitates finding the location of tumors, whereas, at high magnifications, some tiny relevant features for diagnosis could be observed. For example, in the context of breast cancer diagnosis, a higher magnification at 20x could allow one to check nuclear pleomorphism. In contrast, a lower magnification at 5x could allow one to examine tubular formation.

The advances in digital imaging technology allowed traditional tissue slides to be digitized with a Whole Slide Image (WSI) scanner, making the automated diagnosis of histopathological images achievable. However, in practice, most pathologists still used light microscopy to examine the tissue,

\* Correspondence to: School of Computer and Cyber Sciences, Communication University of China, Beijing 100024, China.

\*\* Correspondence to: Guangdong Provincial People's Hospital, Guangdong Academy of Medical Sciences, Guangzhou 510080, China.

E-mail addresses: songmingli@cuc.edu.cn (M. Song), lucheng@gdph.org.cn (C. Lu).

and snapshots of critical field-of-views were captured using mounted cameras for histology examination report or case study. Nevertheless, collections of such snapshots were usually saved without magnification information. The loss of magnification information may hinder the full use of these microscopic snapshots for future research and education, especially those containing valuable organ and disease knowledge. For example, one may want to create a machine learning model to learn the phenotype of a specific disease or to create a histologic image content retrieval system, which required associated magnification information. Therefore, if we want to take full advantage of the valuable knowledge associated with the snapshot images, either from a local hospital report collection, or snapshots collected from research papers, a fundamental premise is to predict the related magnification information accurately.

Recently, deep learning models have been widely used in histopathological image tasks and have achieved satisfactory results because of their strong feature extraction capabilities.<sup>5–7</sup> However, because a few large publicly available digital pathology image datasets contain magnification information, it is difficult to train a reliable deep learning model to predict the magnification level of pathological images accurately. As a result, a dataset with a fine-grained magnification level is needed to train deep learning models, which is also one of the main motivations of this work.

In this paper, we constructed a new dataset, named Hagni40, consisting of 94 643 H&E stained histology image patches at 40 different magnifications of 13 types of cancers which were created from The Cancer Genome Atlas (TCGA) WSIs. Furthermore, we developed a regression model based on a convolutional neural network (CNN) to accurately predict the magnification of a given histology image, named **Histology image magnification finder** (Hagnifinder). We validated the Hagnifinder in Hagni40 for 40 different magnification predictions across 13 different cancers. We also validated the Hagnifinder in a publicly available dataset BreakHis,<sup>8</sup> for 4-level magnification predictions and compared the performance with state-of-the-art methods.

## Literature review of related works

This section reviews some related works on predicting magnification levels and summarizes their similarities and differences with Hagnifinder (**Table 1**).

Eventhough we could have associated magnification levels with high resolution WSIs, we still want to fully utilize those typical and invaluable histology snapshots selected as representative cases in published papers or case reports. Several recent research works proposed automated models for histology image magnification classification. Bayramoglu et al.<sup>9</sup> trained a multi-task CNN to predict malignancy and image magnification levels simultaneously. They declared that networks trained with data with multiple magnification levels performed better than those with a single magnification level. A lightweight multi-task CNN was proposed by Wang et al. to classify the magnification levels and Human epidermal growth factor receptor 2 (Her2) Scores for WSIs.<sup>10</sup> Otálora et al.<sup>11</sup> trained 2 CNN models, one trained to regress the area of pre-segmented nuclei, the other one trained to regress the magnification. They found that a linear combination of these trained models achieved superior performance, with a F1-score of 0.912. Zaveri et al.<sup>12</sup> trained a CNN-based approach using DenseNet121<sup>13</sup> to predict 5 different magnification levels and obtain 93% accuracy. A summary of the methods mentioned above is shown in **Table 1**.

**Table 1**  
Summary of related work.

Methods	Type	Base model	Organ site	Magnification levels
Bayramoglu et al. <sup>9</sup>	Classification	Modified AlexNet	Single (Breast)	4
Otálora et al. <sup>11</sup>	Regression	DenseNet-BC121	Single (Breast)	7
Wang et al. <sup>10</sup>	Classification	Modified AlexNet	Single (Breast)	3
Zaveri et al. <sup>12</sup>	Classification	DenseNet121	Multiple	5
Hagnifinder	Regression	Modified ResNet50	Multiple	40

From **Table 1**, one may observe that most previous methods formulated magnification prediction as a multi-class classification problem, with 3–5 commonly used magnification levels (such as 40x, 20x, 10x, 5x, etc.). In fact, histologic snapshots may be captured at a random magnification, or they are shrank or enlarged unintentionally to fit the page layout. Therefore, an automated model that can accurately predict the magnification is desired. Otálora et al.<sup>11</sup> constructed a regression model, but its predictive outputs are limited to 7 specific magnification levels.

In order to provide a benchmark for different models learning the magnification of histology images, Zaveri et al.<sup>14</sup> have tried to organize a dataset name Kimia-5MAG, consisting of more than 30 000 patches at 5 different magnification levels created from H&E stained WSIs of TCGA. Spanhol et al.<sup>8</sup> published BreakHis dataset consisting of 7909 breast histology images with 4 different magnifications.

Compared with previous methods, we constructed a dataset containing 40 different magnification levels distributed in the range of 1x–40x. This dataset could help us to train a reliable and generalizable model.

## Methodology

In this study, a regression model named Hagnifinder based on deep learning is proposed to predict the magnification level of digital pathological images. An overview of the training and testing processes of Hagnifinder is shown in **Fig. 1**. Hagnifinder is trained using a dataset named Hagni40 containing patches with 40 different magnifications (1x–40x) in the training phase. These patches are collected from 13 different types of solid tumor whole slide images, with sizes ranging from 224 × 224 pixels to 496 × 496 pixels, and at least 60% of the area in each patch is composed of nuclei. In the testing phase, the performance of the Hagnifinder is evaluated by giving a randomly selected patch with unknown magnification, and the absolute value of the difference between the predicted magnification and the truth magnification is used as the evaluation metric.

### Model architecture

Hagnifinder is composed of 3 modules: Feature Extraction Module, Regression Module, and Adaptive Scaling Module (ASM). The entire architecture of the Hagnifinder is shown in **Fig. 2**.

#### Feature extraction module

Recent studies have shown that CNNs have an excellent ability to extract and select features,<sup>15,16</sup> and deep CNNs can learn abstract high-level features from images.<sup>13</sup> ResNet learns features by learning residual representations instead of direct mappings.<sup>17</sup> Compared with ordinary CNN, the advantage of ResNet is that it solves the problem of deep network degradation caused by gradient disappearance or explosion.

#### Regression module

We perform regression on features extracted from pathological images using neural networks to find the quantitative relationship between extracted features and magnifications.

The histopathological images are passed through the Feature Extraction Module, mentioned in the last subsection, and an average pooling layer to obtain feature embeddings. These feature embeddings are then connected with 3 fully connected (FC) layers. These FC layers can increase the nonlinear expression ability, which can theoretically improve the learning

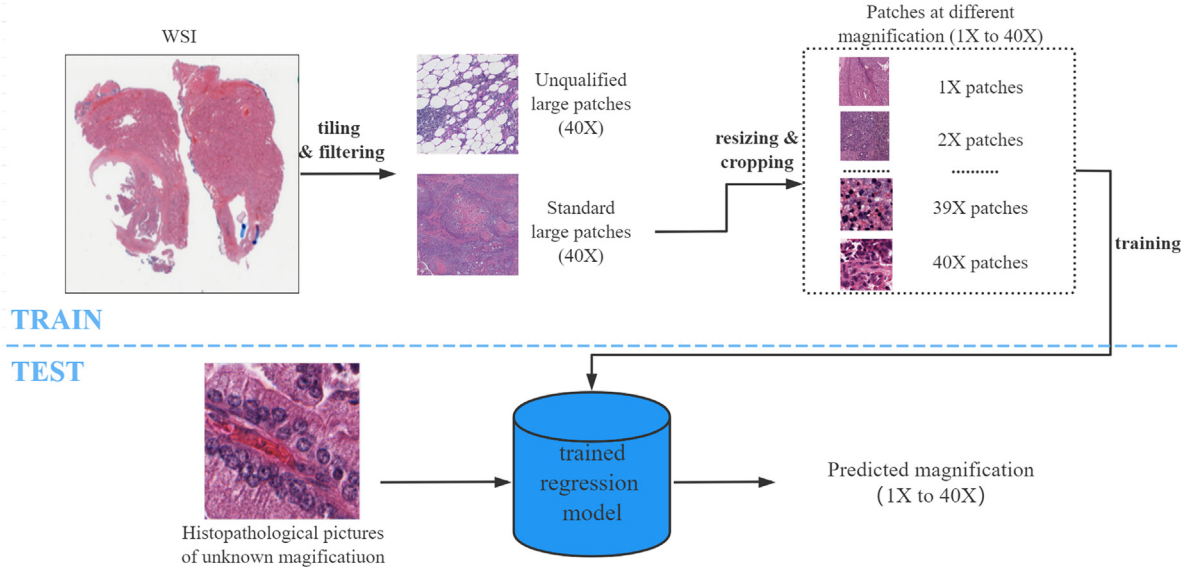


**Fig. 1.** The flowchart of using the Hagnifinder.

ability of the Hagnifinder. The numbers of input nodes of these 3 FC are 2048, 200, and 20, and the numbers of output nodes are 200, 20, and 1, respectively. The final output is a decimal value that denotes the predicted value of the input image's magnification level.

An activation function before the last FC is added, which aims to transform the data nonlinearly and limit the range of data (through mapping the input data to a certain range) to prevent data overflow. Tanh () was chosen as the activation function.

#### Adaptive scaling module

During the training procedure, it is inevitable to encounter problems related to gradient explosion and outliers in feature embeddings, especially in the case of learning embedded features from images at 40 different magnifications. Therefore, the performance of the model cannot be guaranteed, which motivates us to propose an Adaptive Scaling Module in Hagnifinder. The primary purpose of the Adaptive Scaling Module is to regularize the feature embedding representation before it is fed into the nonlinear activation function. In our case, the range of the non-saturated region of the Tanh () function input is  $[-2, 2]$ ; if the embedded feature value is far away from  $[-2, 2]$ , the output value will be close to  $-1$  or  $1$ . In addition, the relative differences of embedded features cannot be reflected in the output. To address the issues mentioned above, the Adaptive Scaling Module makes the embedded feature better distributed in the non-saturated region of the activation function. For each batch of input data  $x$ , the following steps are performed:

**Step 1:** Obtain the maximum absolute value, denoted as  $X$ , from the input data:  $X = \max(|x|)$ ;

**Step 2:** Calculate the variance  $\sigma^2$  of normalized data  $x/X$ .

$$\sigma^2 = \frac{\sum_{i=1}^n (\frac{x_i}{X} - \bar{\frac{x}}{X})^2}{n}. \quad (1)$$

**Step 3:** Set the expected variance  $\hat{\sigma}^2$  to control the distribution of the output data, we set it to 2.2 empirically. The output  $y$  corresponding to this batch of data are as follows:

$$y = x \times \sqrt{\hat{\sigma}^2 / \sigma^2} / X. \quad (2)$$

An example is shown in Fig. 3 below. Let a vector  $[-1, 1, -2, 2, 300]$  represents an embedded feature vector, in which value 300 represents an outlier. Fig. 3 illustrates the outputs of this embedded feature vector if we: (1) sent this vector into Tanh function directly; (2) use normalization operation (i.e., Min-Max Scaling, which linearly transforms the original data, make the output map to the range of  $[0, 1]$ , and achieve equal scaling of the original data) on this vector then sent to Tanh function; (3) use Adaptive Scaling Module on this vector then sent to Tanh function. By comparing the outputs, it is observed that: (1) the absolute differences between all elements are minor if no operation has been applied to the embedded feature vector; (2) by using Min-Max Scaling operation, the output is heavily affected by the outlier so that the first 4 elements are squeezed into a narrow value range; (3) by using the Adaptive Scaling Module, the differences between the first 4 elements can be quantified well while the impact of the outlier (the last element of the vector) is minimized.

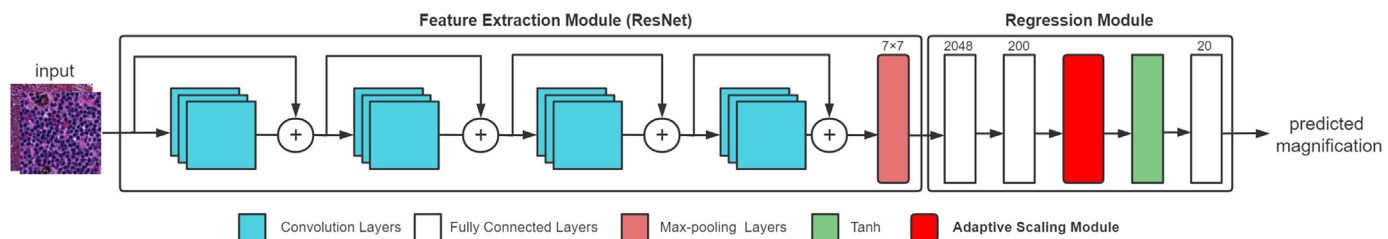


**Fig. 2.** The architecture of the Hagnifinder.

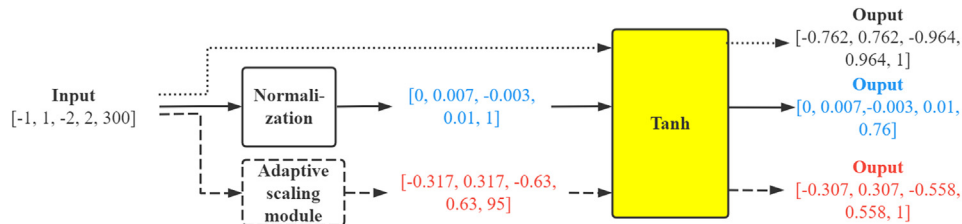


**Fig. 3.** An example demonstrates the functions of ASM. The dotted, solid, and dashed lines represent that the data is sent directly to Tanh, the data is sent to Tanh after normalization processing, and the data is sent to Tanh after passing through ASM, respectively.

### Implementation details

#### Hyper parameters

Hagnifinder was trained with augmented data, in which the input patch was: (1) randomly cropped with a size of (224, 224); (2) rotated with a random angle between  $0^\circ$  and  $90^\circ$ ; (3) flipped horizontally and vertically with a probability of 50%. The model was compiled by the AdamW optimizer, in which the learning rate was set to 0.1. When the training loss did not decrease after 5 consecutive epochs, the learning rate was reduced by 50%. After comparing and verifying through multiple experiments, the expected variance  $\hat{\sigma}^2$  in the Adaptive Scaling Module was set as 2.2.

#### Training strategy

Fig 4 shows the flowchart for training Hagnifinder. The training phase consists of 2 rounds. At first, the Hagnifinder is trained using the strategy described in Fig 4a until it converged (i.e., the training loss did not decrease in the last 10 epochs). Let us assume we have  $n$  batches of training patches. During the first round of training, an average value of the scaling factor  $\bar{m}$  is calculated as follows:

$$\bar{m} = \frac{\sum_{i=1}^n m_i}{n},$$

where

$$m_i = \sqrt{\hat{\sigma}^2 / \sigma^2}.$$

In the second round, shown in Fig. 4b,  $\bar{m}$  is used to replace the Adaptive Scaling Module for training until the model converged.

#### Loss function

We chose Huber Loss as the loss function,<sup>18</sup> which is a piecewise loss function used to solve regression problems. The advantage of Huber Loss

is that it is less sensitive to outliers, so it is not easily affected by outliers. The definition of Huber loss is as follows:

$$L_\delta(y, f(x)) = \begin{cases} \frac{1}{2}(y - f(x))^2, & \text{for } |y - f(x)| \leq \delta \\ \delta \cdot \left(|y - f(x)| - \frac{1}{2}\delta\right), & \text{otherwise.} \end{cases} \quad (3)$$

where  $\delta$  is a parameter that users or experts can set. As shown in Eq. (3), if the prediction deviation is smaller than  $\delta$ , Mean Square Error (MSE) is set as the loss function; whereas if the prediction deviation is larger than  $\delta$ , Mean Absolute Error (MAE) is selected. Huber loss ensures the robustness to abnormal points and ensures the convergence speed of the model.

## Experiments and results

### Dataset construction

The Hagni40 dataset consists of 94 643 patches, which was created by the following steps:

Step 1: WSI selection: We randomly collected 128 H&E stained diagnostic WSIs, at 40x magnification, from 13 different types of cancers from the TCGA. We used HistoQC<sup>19</sup> to control the quality of WSIs.

Step 2: 40x magnification patches generation: Non-overlapped patches with the size of  $2560 \times 2560$  pixels,  $4480 \times 4480$  pixels, and  $8960 \times 8960$  pixels were cropped from all WSIs. A foreground filtering was performed to eliminate the patches containing more than 55% background pixels. This yielded 2445 patches with a size of  $2560 \times 2560$  pixels, 2530 patches of size  $4480 \times 4480$  pixels, and 616 patches of size  $8960 \times 8960$  at 40x magnification.

Step 3: Multi-magnification patches generation: In this step, we performed down-sampling and cropping operations on the 40x magnification patches to obtain patches at different magnifications, i.e., 1x–39x magnification. When generating the down-sampled patches, we limited the size of these patches to smaller than  $500 \times 500$  pixels so that we could process the

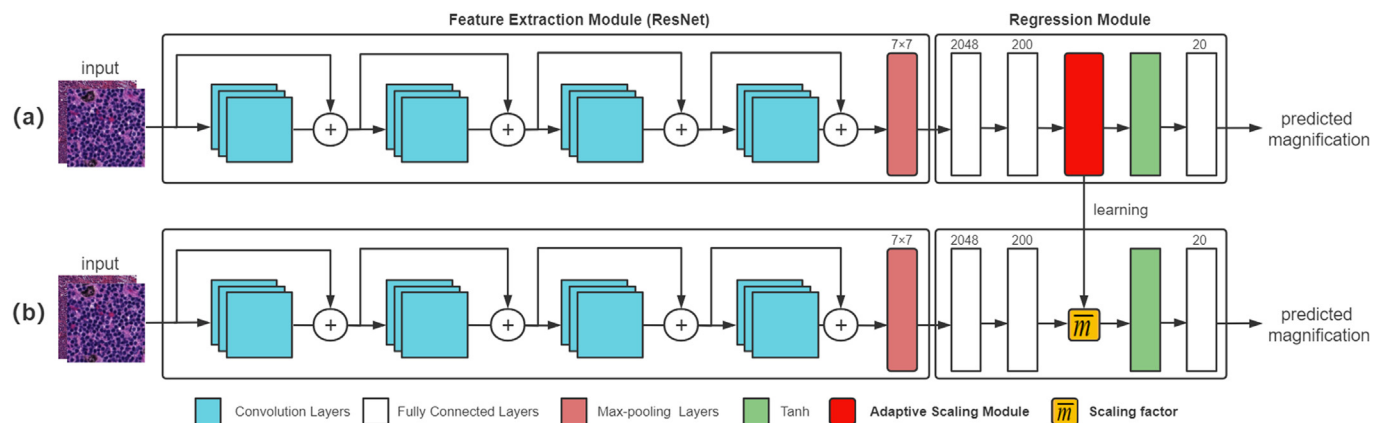


**Fig. 4.** The flow chart of model training.

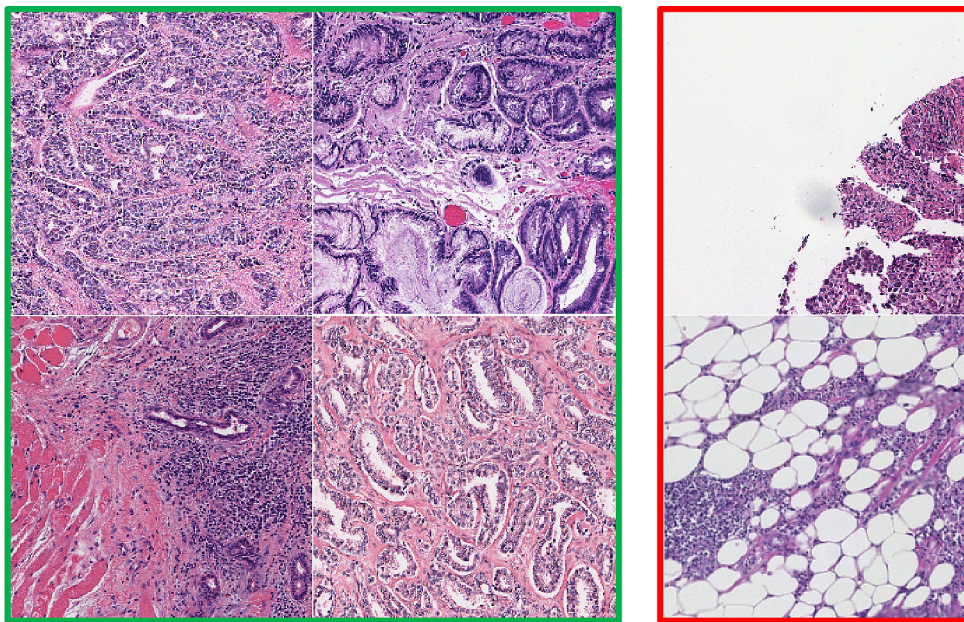


**Fig. 5.** Representative examples of qualified patches, which containing background <40% (green border); and excluded patches, which containing background >40% (red border).

patches in downstream analysis efficiently. We also applied a content filter to eliminate the patches that contained more than 40% of the background (Fig. 5).

At the end, we obtain a high-quality dataset Hagni40, which contains 94 643 patches at 40 different magnification levels. Fig. 6(a) illustrates the magnification distribution of all patches in Hagni40. There are 40 different categories in our dataset that represent 40 different magnification levels, from 1x to 40x. Fig. 6(b) illustrates the magnification distribution across all cancer types.

#### Evaluation metric

In Hagni40 dataset, we randomly select 54 279 patches for training, 18 093 patches for validation, and 18 093 patches for testing. Assume that  $g$  and  $p$  represent the ground truth and predicted magnification for a given image, respectively;  $d$  represents the absolute value of the difference between  $g$  and  $p$ , i. e.  $d = |g - p|$ . Let  $N$  represents the error threshold we set (the maximum error between the predicted value and the ground truth we expect). When  $d > N$ , we consider the prediction of the Hagnifinder under the threshold  $N$  is incorrect, otherwise, the prediction is correct. Let  $CML_N$  indicates the number of images whose magnification predicted by Hagnifinder are correct under the threshold  $N$ , and  $WML_N$  indicates the number of images whose magnification predicted by Hagnifinder are incorrect under the threshold  $N$ . The overall accuracy of Hagnifinder prediction under the threshold  $N$  is defined as follows:

$$ACC_N = \frac{CML_N}{CML_N + WML_N}. \quad (4)$$

#### Performance evaluation

In this evaluation, we randomly split the data into 10 portions based on slide level, in which the first 6 portions were used as training set, 2 portions were used as validation set, and the remaining 2 portions were used as test set. The Hagnifinder was first trained using the training set and then validated using the validation set, followed by test using test set. The performance on test set was reported in this section.

#### Analysis on the performance of Hagnifinder

**Performance of the Hagnifinder with 2 different feature extractors:** In this experiment, we compared the magnification prediction performance of Hagnifinder using Resnet18 and Resnet50 in the Feature Extraction Module. The results of magnification prediction were shown in Table 2, in which we evaluated the ACC at 3 different error thresholds (0.5, 1, and 5). One can observed that the Hagnifinder with deeper convolutional layers for feature extraction, i.e., Resnet50, achieved better performance compared to that of Resnet18. We, therefore, locked down the Hagnifinder with Resnet50 as the feature extractor.

**Magnification prediction accuracy at different magnification levels:** Fig. 7 shows confusion matrices for the Hagnifinder with  $ACC_1$ . Fig. 8 shows the spread of predicted values for different cancer types at each magnification level. It can be seen in Fig. 7 that the Hagnifinder provides consistent prediction accuracy across 40 different magnifications.

To analyze the prediction results from different perspectives, we performed statistical analysis on the prediction results of the magnification levels under different cancer types, as shown in Fig. 9. In terms of the misprediction rate in Fig. 9, we found that the Hagnifinder yield satisfactory performance with misprediction rates less than 5% for all cancer types, and the top 2 highest misprediction rates occurred in the cervical and colon cancers (4.688% and 2.745%, respectively). Fig. 10 presented the sorted misprediction percentages for all magnifications in colon cancer and representative patches from the top misprediction magnifications.

#### Comparison with other methods

To compare the performance of Hagnifinder with other methods, we evaluated all methods on the Hagni40 and a public available dataset named BreakHis.<sup>8</sup> The results were shown in Table 3. In BreakHis dataset, Hagnifinder outperformed the existing methods in terms of accuracy. In Hagni40 dataset, Hagnifinder provided comparable performance with that of the method proposed by Zaveri et al. Note that the Hagnifinder could yield 40 different magnification levels, and we limited the Hagnifinder to 4 magnification levels in order to compare the performance of existing methods.

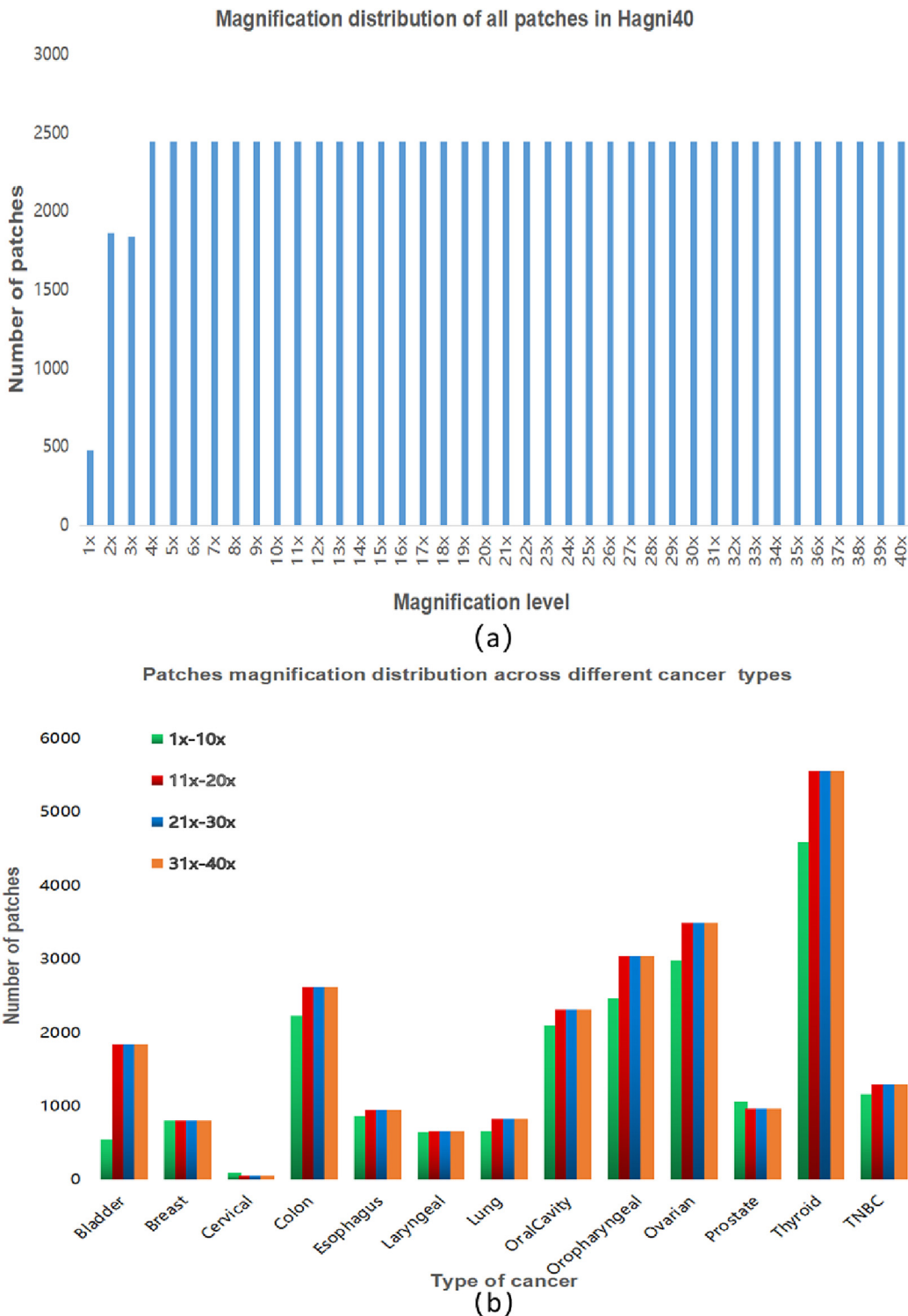


**Fig. 6.** (a) Magnification distribution of all patches in Hagni40. (b) Patches magnification distribution across different cancer types.

## Discussion

More and more artificial intelligent (AI) models have been constructed for cancer diagnosis,<sup>20</sup> prognosis,<sup>21</sup> and mutation prediction<sup>22</sup> using traditional H&E-stained histology images. Training a robust AI model requires many representative cases with labels or annotations, which is difficult to obtain. Fortunately, we have open access to medical databases such as PubMed Central and in-house case reports. We could use the snapshots representing specific disease regions of interest to enrich the training data for

**Table 2**  
Magnification prediction results in the test set of Hagni40.

Feature extractor	ACC <sub>0.5</sub>	ACC <sub>1</sub>	ACC <sub>S</sub>
Resnet18	53.4%	82.80%	99.89%
Resnet50	88.22%	98.89%	100%

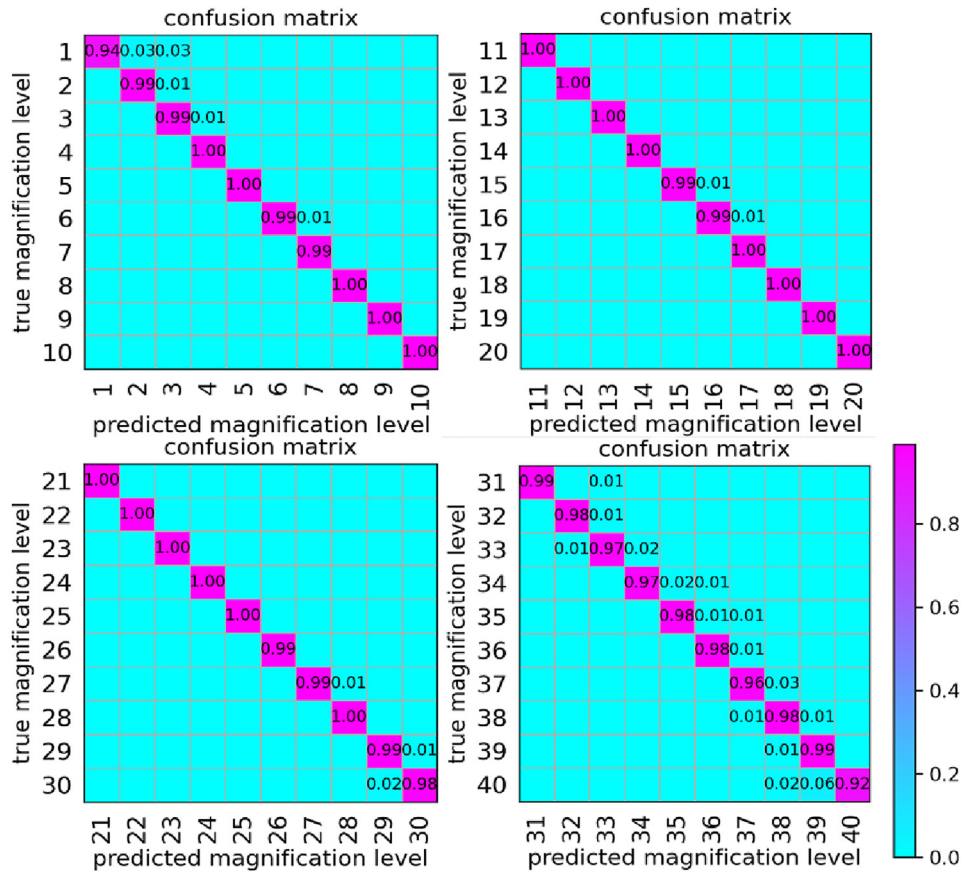


Fig. 7. Confusion matrices for the Hagnifinder.

constructing the AI model. However, these invaluable snapshots are generally saved without magnifications, limiting their usage since the magnification level provides a context to an AI model on what kind of image feature it is learning. Therefore, a robust magnification predictor is required for utilizing those diverse snapshot repositories consisting of different diseases. The Hagnifinder proposed in this work could provide such a functionality: given a random snapshot with a random organ site, providing a predictive magnification level associated with the snapshot.

Several existing works have proposed magnification prediction tools for histology images, either using a classification or regression model.<sup>9-12</sup> Bayramoglu et al., Wang et al., and Otlora et al. trained CNN models for histology image magnification prediction only for breast cancer. Recently, Zaveri et al. presented a model that could predict the magnification of given histology with any disease sites. However, to the best of our knowledge, all existing works reported that they could predict the magnification of histology images up to 7 levels. Note that the snapshots presented on the papers or in the case reports may associate with any magnification levels. Therefore, the Hagnifinder may be a more versatile model for predicting magnification levels, i.e., with 40 magnifications from 1x to 40x and 13 different disease sites.

In the experimental results, one may observe that the Hagnifinder could provide consistent prediction accuracy not only across 40 different magnifications and also across 13 different disease sites. Even though in comparison with other existing methods designed explicitly for 4x, 10x, 20x, and 40x magnification prediction, the Hagnifinder could provide superior or comparable performance in 2 different datasets.

In Fig. 7, we present the confusion matrices for the Hagnifinder across 40 different magnifications. One may observe that the 2 magnifications at the extreme have relatively low accuracy, i.e., 93.5% for 1x magnification and 92.3% for 40x magnification.

The reason could be that they are at the boundary of the magnification-level range (i.e. [1, 40]), which limits the distribution range of the predicted values. Specifically, for a patch with a true magnification level of 20x, the prediction is correct when the predicted value is in the range of [19, 21], while for a patch with true magnification level of 1x or 40x, the predicted value is in the range of [1, 2] or [39, 40], respectively.

In Fig. 9, one may observe that cervical cancer has the highest misprediction rate at 4.688%. This may be because the cervical cancer has the lowest number of patches (see Fig. 6(b), and the number of patches is 314), so the Hagnifinder cannot properly learn cervical histology morphological information well and therefore lead to a relatively high misprediction rate. In the case of colon cancer, Fig. 10(a) illustrates the breakdown of misprediction rate across different magnifications, whereas Fig. 10(b) shows representative patches from the top misprediction magnifications. One can observe that most of the misprediction patches are blur or contain just a few numbers of nuclei, which could be the reason for the high misprediction rate.

## Conclusion

In this paper, we proposed Hagnifinder, a CNN-based regression framework to predict the magnification levels of histopathology images. The proposed model included a new module named Adaptive Scaling Module, which could improve prediction performance by adjusting the data distribution. Furthermore, a new dataset named Hagni40 was constructed for magnification classification is introduced to train and test the Hagnifinder. The dataset contains 94 643 patches belonging to 40 different magnification levels and 13 different cancer types. To validate the performance of the Hagnifinder, we conducted experiments on Hagni40 and BreakHis datasets. The experimental results show that the Hagnifinder with Resnet50

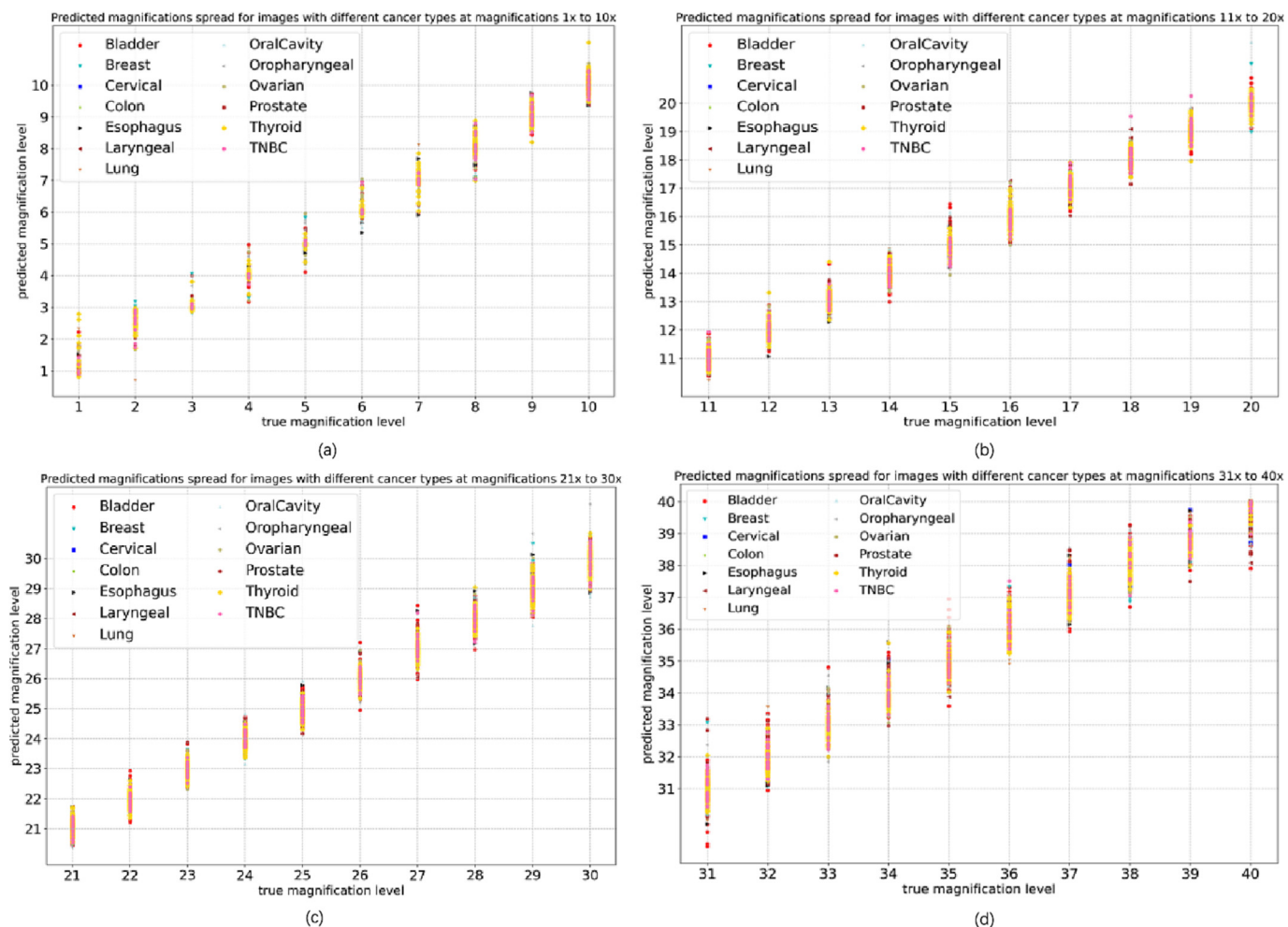


Fig. 8. Spread of predicted values at each magnification level.

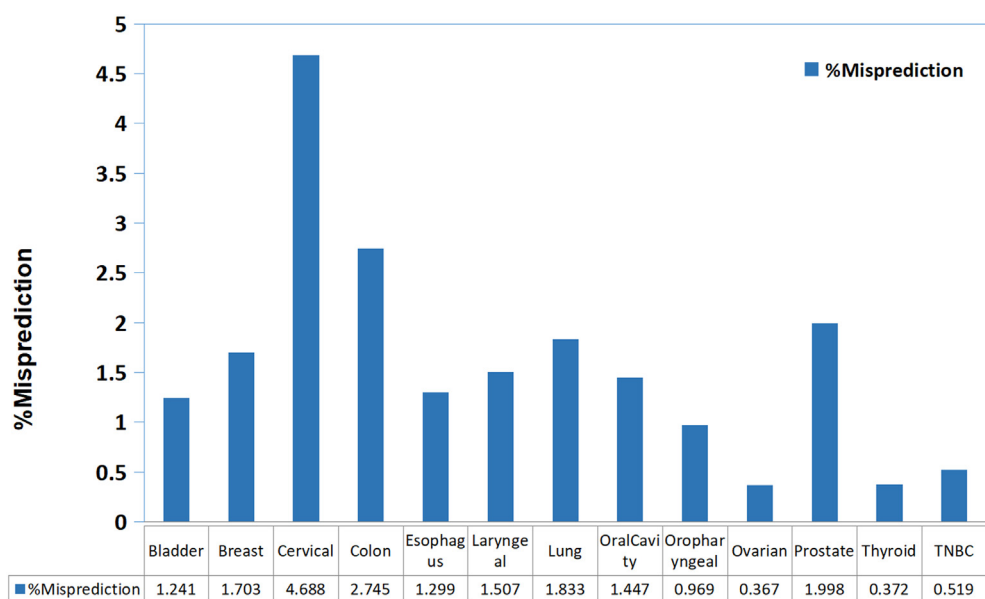
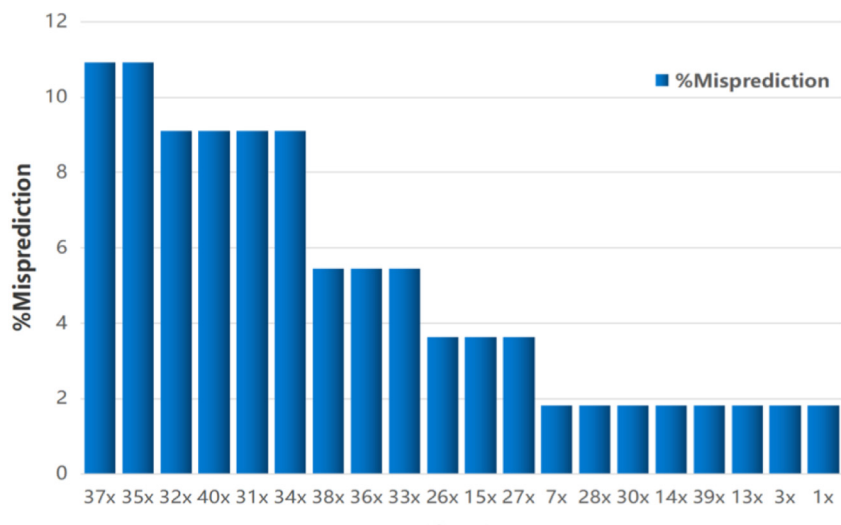
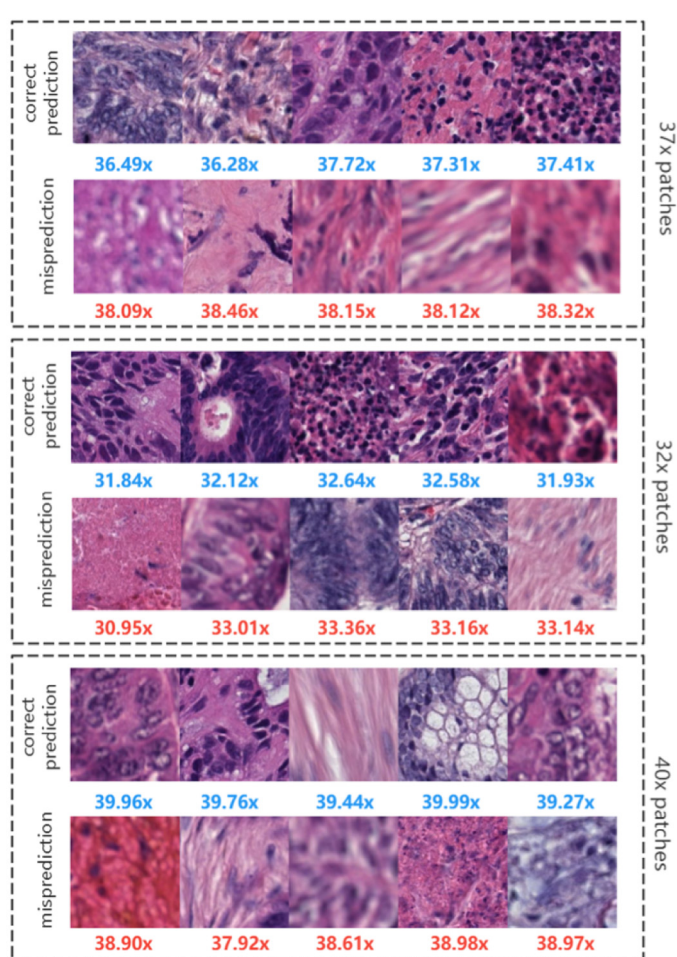


Fig. 9. Number and percentage of mispredictions for each cancer type.



(a)



(b)

**Fig. 10.** (a) Sorted misprediction percentages for all magnifications in colon cancer. (b) Representative patches from the top misprediction magnifications, in which the predicted magnifications were shown under the patches. The comparison between some patches with correct prediction shows that the misprediction is often related to blurry patches or patches with too few nuclei.

**Table 3**

Performance comparison on BreakHis and Hagni40.

Dataset	Methods	Magnification			
		4x	10x	20x	40x
BreakHis	Bayramoglu et al. <sup>9</sup>	84.87%	79.74%	71.72%	84.13%
	Zaveri et al. <sup>12</sup>	97.72%	95.51%	95.17%	96.56%
	Hagnifinder	98.02%	97.41%	95.29%	96.92%
Hagni40	Zaveri et al. <sup>12</sup>	99.14%	98.83%	99.2%	99.19%
	Hagnifinder	100%	99.79%	99.25%	93.29%

as the feature extractor had the best performance on Hagni40 in terms of accuracy (98.9%). The proposed Hagnifinder provided consistent performance across different magnification and cancer types and was superior to the existing methods. The code of Hagnifinder is available at <https://github.com/hacylu/Hagnifinder>. Dataset Hagni40 will be available upon acceptance.

### Competing interest declaration

Dr.'s Liu, Song, and Lu, Mr. Zhang, declare no competing financial interests.

### Acknowledgments

This work was supported by the the National Key R&D Program of China (No. 2021YFF1201003), National Natural Science Foundation of China (No. 61773352 and 82272084), Guangdong Provincial Key Laboratory of Artificial Intelligence in Medical Image Analysis and Application (No. 2022B1212010011), High-level Hospital Construction Project (No. DFJHBF202105), and the Fundamental Research Funds for the Central Universities.

### References

- Veta M, Pluim JPW, Van Diest P.J., Viergever M.A. Breast cancer histopathology image analysis: a review. *IEEE Trans Biomed Eng* 2014;61(5):1400–1411.
- Gurcan MN, Boucheron LE, Can A, Madabhushi A, Rajpoot NM, Yener B. Histopathological image analysis: a review. *IEEE Rev Biomed Eng* 2009;2:147–171.
- Peikari M, Gangeh MJ, Zubovits J, Clarke G, Martel AL. Triaging diagnostically relevant regions from pathology whole slides of breast cancer: a texture based approach. *IEEE Trans Med Imaging* 2016;35(1):307–315.
- Sellarol TL, Filkins R, Hoffman C, Fine JL, Ho J, Parwani AV, et al. Relationship between magnification and resolution in digital pathology systems. *J Pathol Informatics* 2013;4.
- Janowczyk A, Madabhushi A. Deep learning for digital pathology image analysis: a comprehensive tutorial with selected use cases. *J Pathol Informatics* 2016;7.
- Litjens G, Sánchez CL, Timofeeva N, Hermse M, Nagtegaal I, Kovacs I, et al. Deep learning as a tool for increased accuracy and efficiency of histopathological diagnosis. *Scient Rep* 2016;6:26286.
- Gupta V, Bhavsar A. Breast cancer histopathological image classification: is magnification important?. *Computer Vision & Pattern Recognition Workshops. IEEE*; 2017. p. 769–776.
- Spanhol FA, Oliveira LS, Petitjean C, Heutte L. A dataset for breast cancer histopathological image classification. *IEEE Trans Biomed Eng* 2016;63(7):1455–1462.
- Bayramoglu N, Kannala J, Heikkila J. Deep learning for magnification independent breast cancer histopathology image classification. *International Conference on Pattern Recognition. IEEE*; 2017.
- Wang J, Ruan J, He S, Wu C, Ye G, Zhou J, et al. Detection of Her2 scores and magnification from whole slide images in multi-task convolutional network. *International Conference on Pattern Recognition*. 2018.
- Otálora S, Atzori M, Andreczyk V, Müller H. *Image magnification regression using DenseNet for exploiting histopathology open access content. Computational Pathology and Ophthalmic Medical Image Analysis. OMIA COMPAY. Lecture Notes in Computer Science*. 2018.
- Zaveri M, Kalra S, Babaie M, Shah S, Damskinos S, Kashani H, et al. Recognizing magnification levels in microscopic snapshots. *2020 42nd Annual International Conference of the IEEE Engineering in Medicine & Biology Society (EMBC), Montreal, QC, Canada*. 2020:1416–1419.
- Huang G, Liu Z, Laurens V, Kilian Q. Densely Connected Convolutional Networks. *IEEE Computer Society*. 2016.
- Zaveri M, Hemati S, Shah S, Damskinos S, Tizhoosh HR. Kimia-5MA-a dataset for learning the magnification in histopathology images. *IEEE*; 2020.
- Krizhevsky A, Sutskever I, Hinton G. ImageNet classification with deep convolutional neural networks. *Adv Neural Inform Process Syst* 2012;25(2).
- Szegedy C, Liu W, Jia Y, Sermanet J, Reed S, Anguelov D, et al. *Going Deeper with Convolutions. IEEE Computer Society*. 2014.
- He K, Zhang X, Ren S, Sun J. Deep residual learning for image recognition. *Proceedings of the IEEE Conference on Computer Vision and Pattern Recognition (CVPR)*. 2016:770–778.
- Huber PJ. Robust statistics. *J Am Stat Assoc* 2009;78(381):xvi + 354.pp. + loose erratum.
- Janowczyk A, Zuo R, Gilmore H, Feldman M, Madabhushi A. HistoQC: an open-source quality control tool for digital pathology slides. *J Clin Cancer Informatics* 2019;3, 1–7.
- Lu C, Koyuncu C, Corredor G, Prasanna P, Leo P, Wang X, et al. Feature-driven local cell graph (Flock): New computational pathology-based descriptors for prognosis of lung cancer and HPV status of oropharyngeal cancers. *Med Image Anal* 2021;68:101903.
- Lu C, Bera K, Wang X, Prasanna P, Xu J, Janowczyk A, et al. A prognostic model for overall survival of patients with early-stage non-small cell lung cancer: a multicentre, retrospective study. *Lancet Digital Health* 2020;2(11):e594–e606.
- Nicolas C, Santiago OP, Theodore S, Narula N, Snuderl M, Fenyö D, et al. Classification and mutation prediction from non-small cell lung cancer histopathology images using deep learning. *Nat Med* 24 1559–1567 (2018).